DOI: 10.1002/chem.200600219

Neutral Helium Compounds: Theoretical Evidence for a Large Class of Polynuclear Complexes

Stefano Borocci, Nicoletta Bronzolino, and Felice Grandinetti*[a]

Abstract: Ab initio calculations at the MP2 and CCSD(T) levels of theory disclose the conceivable existence of neutral complexes containing up to four helium atoms. These species are formally obtained by replacing the hydrogen atoms of parent molecules such as CH_4, SiH_4, NH_3, PH_3, H_2O, H_2S, C_2H_2, C_2H_4, and C_6H_6 with −NBeHe moieties, which behave as monovalent functional groups containing helium. The geometries and vibrational frequencies of these $M(NBeHe)_n$ ($n>1$; M = central moiety) polyhelium complexes have been investigated at the MP2(full)/6-31G(d) level of theory, and their stability with respect to the loss of helium atom(s) has been evaluated by means of single-point calculations at the CCSD(T)/6-311G(d,p) level of theory. Molecules such as $H_nC(NBeHe)_{4-n}$ and $H_nSi(NBeHe)_{4-n}$ ($n=0$–3), $C_2(NBeHe)_2$, and *ortho*-, *meta*-, and *para*-$C_6H_4(NBeHe)_2$ were invariably characterized as energy minima, and were found to be stable with respect to the loss of helium atom(s) by approximately 4–5 kcal mol^{-1}. On the other hand, species such as $C_2(NBeHe)_4$ and $C_6(NBeHe)_6$ were characterized as high-order saddle points on the potential-energy surface, and were unstable with respect to helium atom(s) loss owing to the bending motion of the −NBeHe groups. The molecules containing N, P, O, or S as the central atom also showed a variable topology and include second-order saddle points such as $S(NBeHe)_2$, third-order saddle points such as $HN(NBeHe)_2$, but also minimum-energy structures such as $O(NBeHe)_2$ and $HP(NBeHe)_2$, which are also stable by approximately 5 kcal mol^{-1} with respect to the helium atom(s) loss. These results suggest the conceivable existence of an, in principle, very large class of $M(NBeHe)_n$ ($n>1$) polyhelium complexes, whose stability may be substantially affected by the nature and the size of the central moiety M. Atoms-in-Molecules (AIM) calculations on selected species invariably suggest that, in our investigated $M(NBeHe)_n$ ($n>1$) compounds, the beryllium–helium interaction is essentially electrostatic.

Keywords: ab initio calculations · atoms-in-molecules (AIM) theory · helium · neutral complexes · stability

Introduction

Since Bartlett's discovery of "$Xe^+PtF_6^-$"[1,2] and the observation of KrF_2 one year later,[3] the chemistry community realized that krypton, xenon, and probably also radon, could have a promising chemistry. Numerous compounds of these elements (xenon in particular) have in fact been subsequently isolated and characterized,[4] and novel evidence of their properties and reactivity is still emerging.[5–11] More recently, another noble gas, argon, was observed in HArF,[12,13] a matrix compound with a strong covalent $(ArH)^+$ bond. In addition, over the years, several neutral complexes such as, for example, $ArW(CO)_5$,[14–16] ArBeO,[17] ArAgX,[18] ArCuX (X = F, Cl, Br),[19,20] ArAuCl,[21] and $CUO(Ar)_n$ ($n \geq 1$)[22] have been experimentally observed in low-temperature matrices. On the other hand, the isolation of neutral species containing helium and neon still remains a fascinating challenge in the chemistry of the lightest noble gases.[23] Helium in particular is the most inert among the inert gases. It has the highest ionization potential (24.587 eV) and the lowest polarizability (0.205 Å^3)[24] of all the chemical elements and therefore appears as a very hard sphere, strongly bound only by positively charged species.[25] As a matter of fact, apart from helium itself, with the formation of He_n ($n \geq 2$) clusters or bulk He,[26] only rare neutral partners such as the Hg atom[27,28] or the cage compound C_{60}[29,30] have been observed to fix helium, and theory is invited to predict the existence of yet unknown compounds and to suggest viable routes to their preparation and structural characterization.

---

[a] Dr. S. Borocci, Dr. N. Bronzolino, Prof. F. Grandinetti
Dipartimento di Scienze Ambientali
Università della Tuscia, L.go dell' Università
s.n.c., 01100 Viterbo (Italy)
Fax: (+39) 0761-357-179
E-mail: fgrandi@unitus.it

Over the years, these calculations have disclosed metastable species such as HHeF,[31–36] $H_3BOBeHe$,[37] and C_6F_5HeF,[38] as well as thermodynamically stable species such as OBeHe[39–41] and SBeHe.[42] More recently, we have found a series of beryllium–helium complexes of general formula RNBeHe.[43] The residue R ranges from the monatomic H, F, and Cl to more complex aliphatic, carbonylic, and aromatic groups, and any species found has been invariably characterized as a minimum-energy structure on the singlet surface, and as stable or metastable with respect to dissociation into He and singlet RNBe. Generally speaking, the −NBeHe moiety behaves as a monovalent "functional group" containing helium, which combines with monovalent residues R− to form a predictably very large class of RNBeHe molecules. This observation suggests the still unexplored possibility that neutral species that contain more than one helium atom do exist. These molecules should have the general formula $M(NBeHe)_n$ ($n>1$), and we studied, in particular, at the ab initio level of theory, the structure and stability of exemplary structures such as $H_nC(NBeHe)_{4-n}$ ($n=0$–2), $H_nN(NBeHe)_{3-n}$ ($n=0$, 1), and $O(NBeHe)_2$, as well as numerous more complex organic molecules that contain up to six −NBeHe groups. Most of the investigated species were actually characterized as true minima on the singlet surface, thus providing the first evidence for stable or metastable polynuclear helium complexes. The details of our calculations will be discussed in the present article.

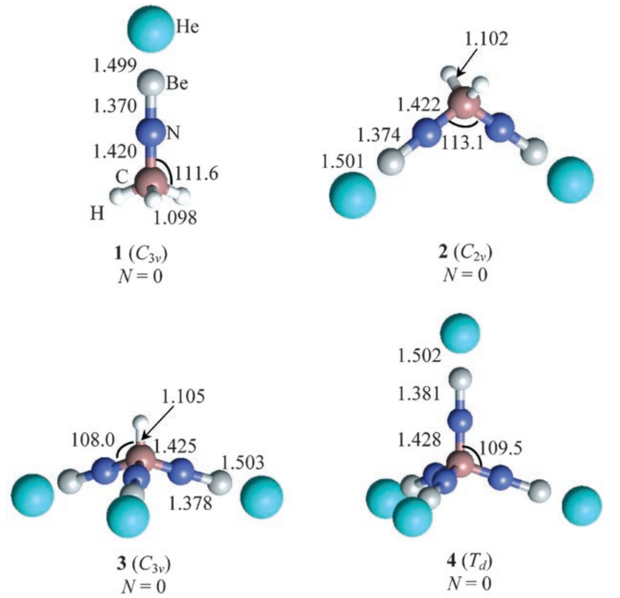

1 (C_{3v})
$N=0$

2 (C_{2v})
$N=0$

3 (C_{3v})
$N=0$

4 (T_d)
$N=0$

Figure 1. MP2(full)/6-31G(d) optimized geometries (bond lengths in Å and bond angles in °) of the $H_nC(NBeHe)_{4-n}$ ($n=0$–3) molecules. N is the number of imaginary frequencies.

Results and Discussion

The presently discussed helium complexes include the group XIV molecules $H_nX(NBeHe)_{4-n}$ ($n=0$–3; X=C, Si), the group XV molecules $H_nX(NBeHe)_{3-n}$ ($n=0$–2; X=N, P), the group XVI molecules HX(NBeHe) and $X(NBeHe)_2$ (X=O, S), and other carbon-containing molecules such as $HC_2(NBeHe)$, $C_2(NBeHe)_2$, $H_nC_2(NBeHe)_{4-n}$ ($n=0$–3), C_6H_5NBeHe, and $C_6H_4(NBeHe)_2$. Their optimized geometries, harmonic frequencies, and thermochemical data, as well as the results of Atoms-in-Molecules (AIM) calculations on selected species, are reported in Figures 1-8 and in Tables 1–8 below.

$H_nX(NBeHe)_{4-n}$ (n=0–3; X=C, Si): The $H_nC(NBeHe)_{4-n}$ molecules **1**–**4** shown in Figure 1 and Table 1, invariably characterized as true minima on the MP2(full)/6-31G(d) potential-energy surface, are indeed exemplary cases among the presently investigated polyhelium complexes.

They are formally obtained by replacing the H atoms of CH_4 with −NBeHe moieties, which behave as monovalent functional groups containing helium. The Be−N and Be−He bond lengths are computed to be around 1.375 and 1.500 Å, respectively, and their corresponding harmonic frequencies all range around 1700 and 500 cm^{-1}, respectively. In addition, the frequency of the N-Be-He bending motions are invariably predicted to be around 150 cm^{-1}. Concerning the

Table 1. MP2(full)/6-31G(d) harmonic vibrational frequencies [cm^{-1}] and CCSD(T)/6-311G(d,p)//MP2(full)/6-31G(d) dissociation energies [kcal mol^{-1}] at 0 K of the $H_nC(NBeHe)_{4-n}$ ($n=0$–3) molecules **1**–**4** (see Figure 1).

	$H_3CNBeHe$ (**1**)[a]	$H_2C(NBeHe)_2$ (**2**)[a]	$HC(NBeHe)_3$ (**3**)[a]	$C(NBeHe)_4$ (**4**)
$\tilde{\nu}$(Be−He)	538.6 (A_1,1.4)[b]	468.8 (A_1,1.1)[b]	456.9 (A_1,0.3)[b]	454.0 (A_1,0)[b]
		537.7 (B_2,7.1)[b]	472.6 (E,0.003)[b]	464.3 (T_2,0.3)[b]
$\tilde{\nu}$(Be−N)	1722.8 (A_1,29.5)[b]	1689.9 (A_1,16.1)[b]	1660.4 (A_1,5.6)[b]	1633.5 (A_1, 0)[b]
		1698.8 (B_2,89.6)[b]	1673.8 (E,104.4)[b]	1649.7 (T_2,102.1)[b]
δ(N-Be-He)	161.0 (E,10.2)[b]	143.9 (A_2,0)[b]	129.7 (A_2,0)[b]	112.0 (T_1,0)[b]
		148.7 (B_2,10.6)[b]	139.6 (E,7.8)[b]	167.0 (E,0)[b]
		157.4 (B_1,19.0)[b]	184.7 (E,0.4)[b]	173.5 (T_2,0.3)[b]
		200.4 (A_1,0.1)[b]	186.8 (A_1,0.01)[b]	
ω(N-Be-He)[c]		89.8 (A_1,22.4)[b]	83.7 (E,19.7)[b]	73.1 (E,0)[b]
			95.3 (A_1,54.1)[b]	84.1 (T_2,49.9)[b]
$\tilde{\nu}$(C−N)	1017.3 (A_1,9.6$_5$)[b]	978.3 (A_1,1.6)[b]	939.7 (A_1,1.9)[b]	759.5 (A_1,0)[b]
		1026.2 (B_2,112.9)[b]	1024.6 (E,177.4)[b]	1035.3 (T_2,245.9)[b]
δ(C-N-Be)	299.9 (E,11.7)[b]	274.4 (B_2,1.4)[b]	259.2 (E,0.5)[b]	261.8 (T_1,0)[b]
		274.7 (B_1,14.0)[b]	270.3 (A_2,0)[b]	
		277.5 (A_2,0)[b]		
δ(N-C-N)		612.1 (A_1,3.8)[b]	585.1 (E,13.6$_5$)[b]	487.8 (E,0)[b]
			678.2 (A_1,0.2)[b]	630.7 (T_2,9.5)[b]
ΔE_1[d]	4.7 (5.5)[e]	4.4 (5.1)[e]		
ΔE_2[f]		4.4 (5.2)[e]		

[a] The -CH_n motions ($n=1$, 2, or 3) are not included. [b] Symmetry and IR intensity [km mol^{-1}] are given in parentheses. [c] (HeBeN)-C-(NBeHe) bending motion. [d] Energy change of Equations (1) and (2). [e] The values in parentheses are not corrected for the BSSE. [f] Energy change of Equation (3).

Table 2. Optimized geometries (bond lengths in Å and bond angles in °), harmonic vibrational frequencies [cm^{-1}], and dissociation energies [kcal mol^{-1}] at 0 K of $H_2C(NBeHe)_2$ (Figure 1, structure **2**).

Method/basis set	C–N[a]	Be–N	Be–He	N-C-N	$\tilde{\nu}$	ΔE_1[b]	ΔE_2[c]
MP2(full)/6-31G(d)	1.422	1.374	1.501	113.1	89.8; 143.9; 148.7; 157.4; 200.4; 274.4; 274.7; 277.5; 468.8; 537.7; 612.1; 978.3; 1026.2; 1077.7; 1285.7; 1399.6; 1556.5; 1689.9; 1698.8; 3021.6; 3055.8	3.0 (4.3)[d]	3.0 (4.3)[d]
MP2(full)/6-311G(d,p)	1.423	1.375	1.489	112.8		4.3 (5.2)[d]	4.3 (5.2)[d]
MP2(full)/6-311++G(2df,2p)	1.417	1.372	1.491	113.1		4.7 (5.5)[d]	4.7 (5.5)[d]
CCD/6-31G(d)	1.425	1.360	1.507	114.0	89.9; 147.9; 150.2; 161.6; 211.1; 278.5; 287.1; 287.6; 471.4; 535.1; 619.3; 990.7; 1057.9; 1081.7; 1289.0; 1414.0; 1554.4; 1772.4; 1774.3; 2983.1; 3002.4	3.0 (4.2)[d]	3.0 (4.2)[d]
CCD/6-311G(d,p)	1.426	1.357	1.503	114.0		4.0 (4.8)[d]	4.0 (4.8)[d]
CCSD(T)/6-311G(d,p)	1.430	1.369	1.495	113.7		4.4 (5.2)[d]	4.4 (5.2)[d]

[a] The C–H bond length and the H-C–H bond angle range from 1.096 Å (MP2(full)/6-311++G(2df,2p)) to 1.106 Å (CCSD(T)/6-311G(d,p)) and from 106.0° (CCD/6-31G(d)) to 106.8° (MP2(full)/6-311G(d,p)), respectively. [b] Energy change of Equation (2). [c] Energy change of Equation (3). [d] The values in parentheses are not corrected for the BSSE.

accuracy of these MP2(full)/6-31G(d) geometries and frequencies, we note that the CCSD(T)/6-311G(d,p) T1 diagnostics of **1** and **2** are within the threshold of 0.02 usually accepted to support the validity of a monodeterminantal description of the wave function, and that the MP2(full)/6-31G(d) geometry of **1** is in very good agreement with the CCSD(T)/6-311G(d,p) parameters (C–N: 1.426 Å; Be–N: 1.367 Å; Be-He: 1.493 Å) obtained in our previous work.[43] In addition, the presently performed test calculations on **2**, reported in Table 2, reveal that its MP2(full)/6-31G(d) bond lengths deviate from the CCSD(T)/6-311G(d,p) values by only approximately 0.05 Å and that the N-C-N bond angle differs by only 0.6°. Finally, the MP2(full)/6-31G(d) harmonic frequencies are in qualitative and also quantitative agreement with those obtained at the CCD/6-31G(d) level of theory.

The predicted thermochemistry of **1** and **2** confirms that the −NBeHe groups of $H_nC(NBeHe)_{4-n}$ ($n=0$–3) are indeed essentially independent functional groups. The CCSD(T)/6-311G(d,p)//MP2(full)/6-31G(d) energy changes at 0 K of the reactions shown in Equations (1) and (2) are in fact quite similar (see Table 1), and, irrespective of the employed computational level (see Table 2), the ΔE of the reaction shown in Equation (2), 4.4 kcal mol^{-1}, is coincident with the energy change of the dissociation shown in Equation (3).

$$\mathbf{1} \rightarrow H_3CNBe + He \tag{1}$$

$$\mathbf{2} \rightarrow H_2C(NBeHe)NBe + He \tag{2}$$

$$H_2C(NBeHe)NBe \rightarrow H_2C(NBe)_2 + He \tag{3}$$

Concerning the nature of the beryllium–helium interaction in complexes **1**–**4**, the MP2(full)/6-311G(d,p) AIM analyses of **1** and **2** suggest that it is essentially electrostatic. We note in fact from Figure 2 and Table 3 that in both these species the charge transfer from helium to beryllium is practically negligible, if present at all, and that the Laplacian of the electron density ($\nabla^2\rho$) at the bond critical point located on the attractor interaction line corresponding to the Be–He bond is positive and computed as approximately +8.3 e Å^{-5}. These results are quite similar to those obtained previously for other beryllium–helium complexes such as OBeHe,[39–41] SBeHe,[42] and H$_3$BOBeHe.[37]

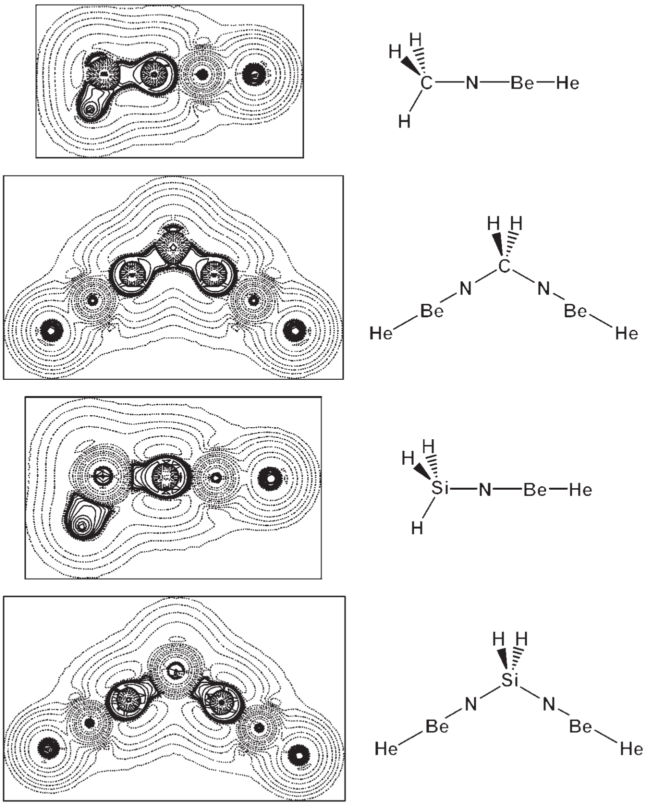

Figure 2. Contour line diagrams of the MP2(full)/6-311G(d,p) Laplacian of the electronic charge density $-\nabla^2\rho(\mathbf{r})$ (in the σ_v plane) of H$_3$CNBeHe, H$_2$C(NBeHe)$_2$, H$_3$SiNBeHe, and H$_2$Si(NBeHe)$_2$. Dashed lines are in regions of charge depletion ($-\nabla^2\rho(\mathbf{r})<0$) and solid lines in regions of charge concentration ($-\nabla^2\rho(\mathbf{r})>0$).

The salient features of the $H_nSi(NBeHe)_{4-n}$ complexes **5**–**8**, displayed in Figure 3 and Table 4, closely resemble those of their carbon analogues **1**–**4**.

All these structures have in fact been characterized as true minima on the MP2(full)/6-31G(d) potential-energy surface, and their −NBeHe moieties are again recognizable

Table 3. MP2(full)/6-311G(d,p) Atoms-in-Molecules (AIM) analysis of selected helium complexes.

Species	$q(X)$[a,b]	$q(N)$[a]	$q(Be)$[a]	$q(He)$[a]	Bond	ρ[c]	$\nabla^2\rho$[d]
$H_3CNBeHe$	0.442	−1.880	1.491	−0.039	C−N	1.876	−18.894
					N−Be	1.005	30.847
					Be−He	0.209	8.314
$H_2C(NBeHe)_2$	0.839	−1.860	1.476	−0.041	C−N	1.883	−19.351
					N−Be	0.992	30.292
					Be−He	0.209	8.266
$H_3SiNBeHe$	2.933	−2.284	1.558	−0.028	Si−N	0.884	16.315
					N−Be	1.019	28.847
					Be−He	0.209	7.856
$H_2Si(NBeHe)_2$	3.013	−2.267	1.531	−0.033	Si−N	0.864	15.929
					N−Be	1.012	28.654
					Be−He	0.202	7.856
$H_2NNBeHe$	−0.619	−1.456	1.422	−0.041	N−N	2.274	−15.206
					N−Be	0.965	30.726
					Be−He	0.209	8.579
$H_2PNBeHe$	1.859	−2.180	1.525	−0.034	P−N	1.107	10.338
					N−Be	1.005	29.425
					Be−He	0.209	8.121
HONBeHe	−0.694	−1.283	1.450	−0.038	O−N	2.281	−13.013
					N−Be	0.958	31.208
					Be−He	0.216	8.652
HSNBeHe	0.579	−1.946	1.491	−0.039	S−N	1.397	−2.844
					N−Be	0.985	30.003
					Be−He	0.216	8.362
C_6H_5NBeHe	0.485	−1.913	1.522	−0.033	C−N	2.051	−20.002
					N−Be	0.999	30.124
					Be−He	0.216	8.266
HO-C_6H_4-(NBeHe)	0.487	−1.915	1.517	−0.035	C−N	2.051	−19.954
					N−Be	0.999	30.148
					Be−He	0.216	8.266
NC-C_6H_4-(NBeHe)	0.509	−1.908	1.543	−0.029	C−N	2.085	−20.460
					N−Be	0.999	30.027
					Be−He	0.216	8.266

[a] AIM formal charge [e]. [b] X is the atom bound to the −NBeHe group. [c] Charge density [$e\,Å^{-3}$] at the bond critical point on the specified bond. [d] Laplacian of the charge density [$e\,Å^{-5}$] at the bond critical point on the specified bond.

as practically independent functional groups, with very similar Be−N and Be−He bond lengths. In addition, the AIM analyses of **5** and **6**, shown in Figure 2 and Table 3, confirm that the beryllium–helium interaction is still essentially electrostatic. The charge transfer from He to Be is practically negligible, and the Laplacian of the electron density ($\nabla^2\rho$) at the bond critical point located on the attractor interaction line corresponding to the Be−He bond is positive and computed as approximately $+7.9\,e\,Å^{-5}$. However, despite the qualitative similarities between **1**–**4** and **5**–**8**, it is still possible to note quantitative differences in their structure and stability that are ascribable to the difference in electronegativity of the central carbon or silicon atom. The Be−N and Be−He bond lengths of any $H_nC(NBeHe)_{4-n}$ ($n=0$–3) molecule are invariably shorter than those of its silicon analogue by approximately 0.01 Å, the corresponding harmonic frequencies are consistently lower, and the CCSD(T)/6-311G(d,p)//MP2(full)/6-31G(d) energy changes at 0 K of the dissociations shown in Equations (4)–(6) are lower than the corresponding reactions shown in Equations (1)–(3) by approximately 0.5 kcal mol^{-1}.

$$\mathbf{5} \rightarrow H_3SiNBe + He \quad (4)$$

$$\mathbf{6} \rightarrow H_2Si(NBeHe)NBe + He \quad (5)$$

$$H_2Si(NBeHe)NBe \rightarrow H_2Si(NBe)_2 + He \quad (6)$$

In any case, their absolute values still range around 4 kcal mol^{-1} and support the prediction that both $H_nC(NBeHe)_{4-n}$ and $H_nSi(NBeHe)_{4-n}$ ($n=0$–3) could be observable, for example, under low-temperature matrix-isolation conditions.

$H_nX(NBeHe)_{3-n}$ (n=0–2; X=N, P), HY(NBeHe), and Y-(NBeHe)$_2$ (Y=O, S): The conceivable existence of a large class of $M(NBeHe)_n$ ($n>1$) polyhelium complexes and the occurrence of periodic trends in their structure and stability was further investigated by studying the nitrogen, phosphorus, oxygen, and sulfur exemplary molecules $H_nX(NBeHe)_{3-n}$ ($n=0$–2; X=N, P), HY(NBeHe), and Y(NBeHe)$_2$ (Y=O, S). The obtained results, shown in

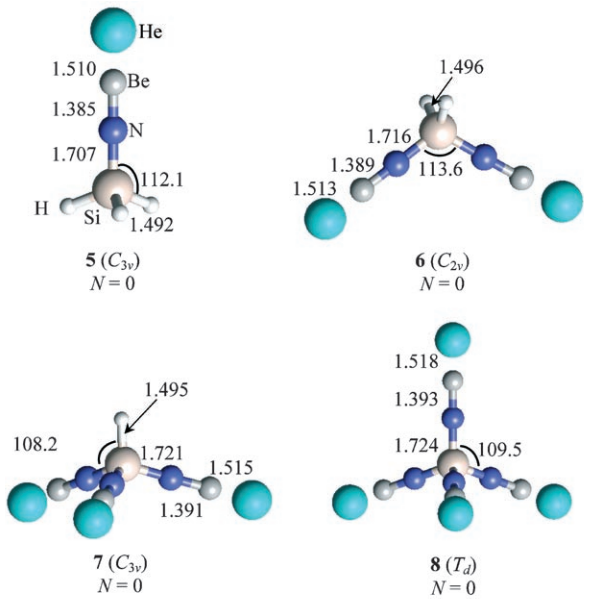

5 (C_{3v}) $N=0$ **6** (C_{2v}) $N=0$ **7** (C_{3v}) $N=0$ **8** (T_d) $N=0$

Figure 3. MP2(full)/6-31G(d) optimized geometries (bond lengths in Å and bond angles in °) of the $H_nSi(NBeHe)_{4-n}$ ($n=0$–3) molecules. N is the number of imaginary frequencies.

Table 4. MP2(full)/6-31G(d) harmonic vibrational frequencies [cm^{-1}] and CCSD(T)/6-311G(d,p)//MP2(full)/6-31G(d) dissociation energies [kcal mol^{-1}] at 0 K of the $H_nSi(NBeHe)_{4-n}$ (n=0–3) molecules **5–8** (see Figure 3).

	$H_3SiNBeHe$ (**5**)[a]	$H_2Si(NBeHe)_2$ (**6**)[a]	$HSi(NBeHe)_3$ (**7**)[a]	$Si(NBeHe)_4$ (**8**)
$\tilde{\nu}$(Be−He)	500.2 (A_1,9.4)[b]	486.1 (A_1,16.7)[b]	489.2 (A_1,30.9)[b]	420.4 (A_1,0)[b]
		497.4 (B_2,22.3)[b]	494.7 (E,41.6)[b]	500.8 (T_2,83.8)[b]
$\tilde{\nu}$(Be−N)	1641.5 (A_1,222.6)[b]	1618.4 (A_1,86.6)[b]	1597.9 (A_1,25.3)[b]	1578.6 (A_1,0)[b]
		1626.8 (B_2,336.6)[b]	1611.4 (E,275.1)[b]	1597.8 (T_2,217.6)[b]
δ(N-Be-He)	140.4 (E,9.7)[b]	135.5 (B_2,5.9)[b]	130.6 (A_2,0)[b]	128.1 (T_1,0)[b]
		135.6 (A_2,0)[b]	133.8 (E,4.3)[b]	175.6 (E,0)[b]
		139.9 (B_1,18.5)[b]	186.6 (E,0.01)[b]	181.6 (T_2,0.04)[b]
		198.5 (A_1,1.7)[b]	195.8 (A_1,3.3)[b]	
ω(N-Be-He)[c]		72.0 (A_1,26.3)[b]	69.6 (E,16.8)[b]	65.2 (E,0)[b]
			79.3 (A_1,56.1)[b]	77.2 (T_2,38.9)[b]
$\tilde{\nu}$(Si−N)	797.6 (A_1,59.8)[b]	748.0 (A_1,33.5)[b]	713.3 (A_1,15.2)[b]	670.9 (A_1,0)[b]
		803.3 (B_2,173.1)[b]	784.4 (E,182.6)[b]	781.0 (T_2,348.3)[b]
δ(Si-N-Be)	235.9 (E,18.7)[b]	224.1 (B_1,19.1)[b]	220.7 (A_2,0)[b]	216.4 (T_1,0)[b]
		227.8 (B_2,3.9)[b]	222.1 (E,1.6)[b]	
		230.4 (A_2,0)[b]		
δ(N-Si-N)		347.8 (A_1,28.8)[b]	332.8 (E,27.0)[b]	311.2 (E,0)[b]
			393.1 (A_1,19.4)[b]	365.6 (T_2,41.0)[b]
ΔE_1[d]	4.3 (5.1)[e]	3.8 (4.6)[e]		
ΔE_2[f]		3.8 (4.6)[e]		

[a] The $-SiH_n$ motions (n=1, 2, or 3) are not included. [b] Symmetry and IR intensity [km mol^{-1}] are given in parentheses. [c] (HeBeN)-Si-(NBeHe) bending motion. [d] Energy change of Equations (4) and (5). [e] The values in parentheses are not corrected for the BSSE. [f] Energy change of Equation (6).

Figure 4 and in Tables 5 and 6, confirm these expectations and also disclose a variability in the topology of the located structures according to the nature of the central atom (N, P, O, or S).

Similar to the carbon and silicon complexes **1–4** and **5–8**, the two oxygen species HONBeHe (**11**) and O(NBeHe)$_2$ (**12**) were characterized as true minima on the MP2(full)/6-31G(d) potential-energy surface, with easily recognizable −NBeHe functional groups featuring quite similar Be−N and Be−He bond lengths and corresponding harmonic frequencies. In addition, consistent with the more electronegative character of oxygen with respect to carbon and silicon, the Be−N and Be−He bond lengths of **11** and **12**, computed as approximately 1.36 and 1.49 Å, respectively, are slightly shorter than those of **1–4** and **5–8**, and the CCSD(T)/6-311G(d,p)//MP2-(full)/6-31G(d) energy changes at 0 K of the reactions shown in Equations (7)–(9), estimated as approximately 5.0 kcal mol^{-1}, are consistently slightly higher than those found for the reactions shown in Equations (1)–(3) and (4)–(6).

$$\mathbf{11} \rightarrow \mathrm{HONBe} + \mathrm{He} \quad (7)$$

$$\mathbf{12} \rightarrow \mathrm{O(NBeHe)NBe} + \mathrm{He} \quad (8)$$

$$\mathrm{O(NBeHe)NBe} \rightarrow \mathrm{O(NBe)_2} + \mathrm{He} \quad (9)$$

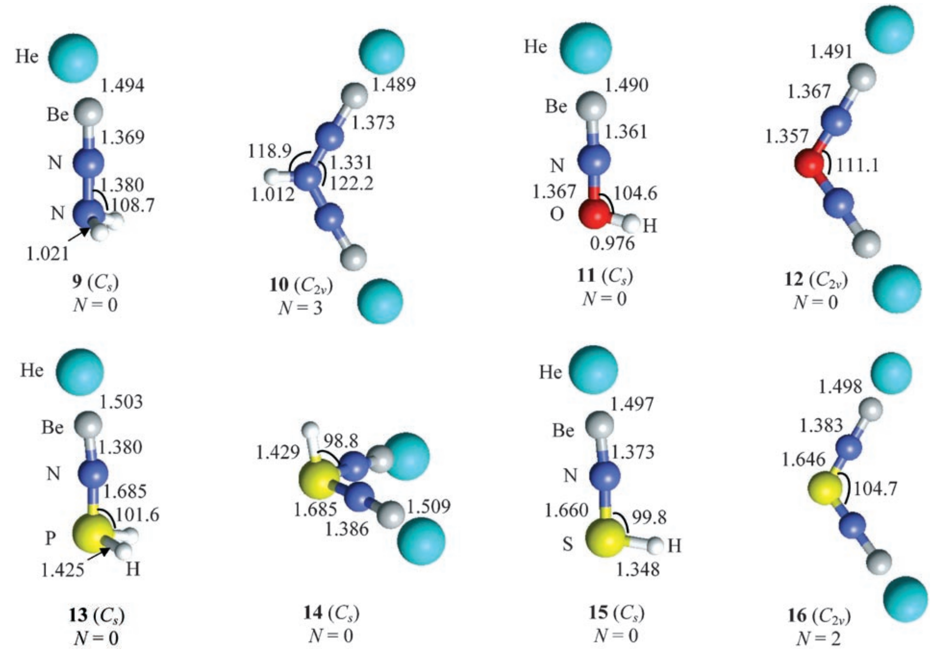

Figure 4. MP2(full)/6-31G(d) optimized geometries (bond lengths in Å and bond angles in °) of the $H_2XNBeHe$, $HX(NBeHe)_2$ (X=N, P), HYNBeHe, and $Y(NBeHe)_2$ (Y=O, S) molecules. N is the number of imaginary frequencies.

On going from oxygen to the less-electronegative sulfur, the monosubstituted species HSNBeHe (**15**), again located as a minimum on the MP2-(full)/6-31G(d) potential-energy surface, has Be−N and Be−He bond lengths and harmonic frequencies that are predictably slightly longer and slightly lower, respectively, than the corresponding values of **11**. In addition, the energy change of the dissociation shown in Equation (10) is consistently slightly lower than that for the reaction shown in Equation (7).

$$\mathbf{15} \rightarrow \mathrm{HSNBe} + \mathrm{He} \quad (10)$$

On the other hand, the disubstituted species S(NBeHe)$_2$ (**16**), although located as a stationary point on the MP2(full)/6-31G(d) potential-energy surface, was characterized as a

Table 5. MP2(full)/6-31G(d) harmonic vibrational frequencies [cm^{-1}] and CCSD(T)/6-311G(d,p)//MP2(full)/6-31G(d) dissociation energies [kcal mol^{-1}] at 0 K of the $H_2XNBeHe$ (X=N, P) and $HP(NBeHe)_2$ molecules **9**, **13**, and **14** (see Figure 4).

	$H_2NNBeHe$ (**9**)[a] (X=N)	$H_2PNBeHe$ (**13**)[a] (X=P)	$HP(NBeHe)_2$ (**14**)[a]
$\tilde{\nu}$(Be−He)	547.2 (A′,0.3)[b]	505.9 (A′,10.7)[b]	495.9 (A″,40.2)[b] 501.4 (A′,14.1)[b]
$\tilde{\nu}$(Be−N)	1695.2 (A′,7.0)[b]	1643.0 (A′,107.8)[b]	1603.5 (A′,37.4)[b] 1612.2 (A″,175.3)[b]
δ(N-Be-He)	100.4 (A′,46.7$_5$)[b]	142.9 (A′,9.7)[b]	121.3 (A″,2.1)[b]
	179.9 (A″,24.1)[b]	147.5 (A″,9.3)[b]	123.9 (A′,21.1)[b] 139.8 (A″,6.2)[b] 189.8 (A′,1.3)[b]
ω(N-Be-He)[c]			73.2 (A′,24.9)[b]
$\tilde{\nu}$(X−N)	957.8 (A′,181.2)[b]	783.7 (A′,74.3)[b]	746.5 (A′,16.4)[b] 765.2 (A″,229.9)[b]
δ(X-N-Be)	334.3 (A″,6.8)[b] 353.1 (A′,4.3)[b]	253.2 (A″,22.0)[b] 260.3 (A′,15.0)[b]	239.2 (A″,11.9)[b] 244.0 (A″,0.8)[b] 247.5 (A′,22.6)[b]
δ(N-P-N)			382.3 (A′,13.0)[b]
Δ*E*[d]	5.6 (6.4)[e]	4.3 (5.1)[e]	

[a] The $-NH_2$ and $-PH_n$ motions ($n=1$ or 2) are not included. [b] Symmetry and IR intensity [km mol^{-1}] are given in parentheses. [c] (HeBeN)-P-(NBeHe) bending motion. [d] Energy change of Equation (11). [e] The values in parentheses are not corrected for the BSSE.

Table 6. MP2(full)/6-31G(d) harmonic vibrational frequencies [cm^{-1}] and CCSD(T)/6-311G(d,p)//MP2(full)/6-31G(d) dissociation energies [kcal mol^{-1}] at 0 K of the HXNBeHe (X=O, S) and $O(NBeHe)_2$ molecules **11**, **12**, and **15** (see Figure 4).

	HONBeHe (**11**)[a] (X=O)	$O(NBeHe)_2$ (**12**)	HSNBeHe (**15**)[a] (X=S)
$\tilde{\nu}$(Be−He)	548.7 (A′,0.3)[b]	489.9 (A_1,2.7)[b] 552.0 (B_2,0.02)[b]	513.3 (A′,2.4)[b]
$\tilde{\nu}$(Be−N)	1722.6 (A′,18.4)[b]	1663.9 (B_2,29.9)[b] 1681.4 (A_1,6.2)[b]	1644.8 (A′,19.0)[b]
δ(N-Be-He)	143.3 (A″,26.8)[b]	107.2 (A_2,0)[b]	122.8 (A″,16.4)[b]
	168.0 (A′,8.7)[b]	115.0 (B_1,32.0)[b] 156.4 (B_2,3.2)[b] 214.1 (A_1,0.07)[b]	151.1 (A′,7.6)[b]
ω(N-Be-He)[c]		92.5 (A_1,24.1)[b]	
$\tilde{\nu}$(N−X)	991.6 (A′,78.1)[b]	927.2 (A_1,30.2)[b] 988.8 (B_2,45.8)[b]	793.3 (A′,8.0)[b]
δ(X-N-Be)	347.7 (A′,10.6)[b]	315.1 (B_2,3.5)[b]	264.7 (A′,21.4)[b]
	372.2 (A″,0.4)[b]	326.4 (A_2,0)[b] 353.4 (B_1,0.9)[b]	282.9 (A″,11.5)[b]
δ(N-O-N)		655.9 (A_1,0.8)[b]	
ΔE_1[d]	5.2 (6.0)[e]	5.0 (5.8)[e]	5.1 (5.9)[e]
ΔE_2[f]		5.0 (5.8)[e]	

[a] The −XH motions (X=O, S) are not included. [b] Symmetry and IR intensity [km mol^{-1}] are given in parentheses. [c] (HeBeN)-O-(NBeHe) bending motion. [d] Energy change of Equations (7), (8), and (10). [e] The values in parentheses are not corrected for the BSSE. [f] Energy change of Equation (9).

second-order saddle point, unstable with respect to the loss of both helium atoms owing to the bending motion of the N-Be-He groups (the two imaginary frequencies are 97.4i and 107.8i cm^{-1}). These results first disclose the possibility that the $M(NBeHe)_n$ ($n>1$) polyhelium complexes may be unstable with respect to helium atom loss, and, at variance with the monosubstituted species RNBeHe, that they cannot be safely predicted as minimum-energy structures on the potential-energy surface. The results on the $H_2X(NBeHe)$, $HX(NBeHe)_2$, and $X(NBeHe)_3$ molecules (X=N, P) confirm this variability in the topology of the $M(NBeHe)_n$ species. In fact, both $H_2N{-}NBeHe$ (**9**) and $H_2P{-}NBeHe$ (**13**) were located to be true minima on the MP2(full)/6-31G(d) potential-energy surface, with differences in the Be−N and Be−He bond lengths and harmonic frequencies that parallel the difference in the electronegativity of N and P. In addition, the CCSD(T)/6-311G(d,p)//MP2(full)/6-31G(d) energy change of the reaction shown in Equation (11) is slightly higher for X=N.

$$H_2X{-}NBeHe \rightarrow H_2X{-}NBe + He \qquad (X = N, P) \tag{11}$$

Both $HN(NBeHe)_2$ (**10**) and $HP(NBeHe)_2$ (**14**) have also been located as stationary points on the potential-energy surface. However, only **14** was characterized as a true energy minimum, whereas the nitrogen-containing species **10** revealed a third-order saddle point, and was unstable with respect to the out-of-plane bending motion of the H atom (imaginary frequency: 644.4i cm^{-1}), and to two nearly degenerate bending motions of the N-Be-He groups (imaginary frequencies: 224.1i and 224.8i cm^{-1}). The instability of the HP(NBeHe)NBe fragment on the MP2(full)/6-31G(d) potential-energy surface prevented the evaluation of the helium fixation energy in **14**. Finally, despite careful searching, we did not locate any stationary point corresponding to the trisubstituted structures $N(NBeHe)_3$ and $P(NBeHe)_3$.

Organic polyhelium complexes: Following the investigation of exemplary $M(NBeHe)_n$ polyhelium complexes containing a single central atom, we searched for structures containing two or more −NBeHe functional groups bound to larger organic skeletons. We focused first on the $HC_2(NBeHe)$, $C_2(NBeHe)_2$, and $H_nC_2(NBeHe)_{4-n}$ ($n=0$–3) molecules shown in Figures 5 and 6, the results for which are shown in Table 7.

All these species were located as stationary points on the MP2(full)/6-31G(d) potential-energy surface, with clearly recognizable −NBeHe functional groups featuring typical Be−N and Be−He bond lengths of approximately 1.38 and 1.50 Å, respectively, and corresponding harmonic frequencies of around 1700 and 500 cm^{-1}, respectively. However, at variance with the carbon complexes **1**–**4** but similar, for example, to the nitrogen and sulfur molecules **9**, **10** and **13**–**16**, the complexes **17**–**24** showed a variability in their topology related to the number of −NBeHe substituents. First, both the monosubstituted molecules **17** and **23** were confirmed to be energy minima on the singlet surface, stable with respect to helium atom loss by 4.9 and 5.3 kcal mol^{-1}, respectively, at the CCSD(T)/6-311G(d,p)//MP2(full)/6-31G(d) level of theory at 0 K (see Table 7). These dissociation energies are slightly higher than the saturated compound **1** (4.7 kcal mol^{-1}) and their trend parallels the increasing electronega-

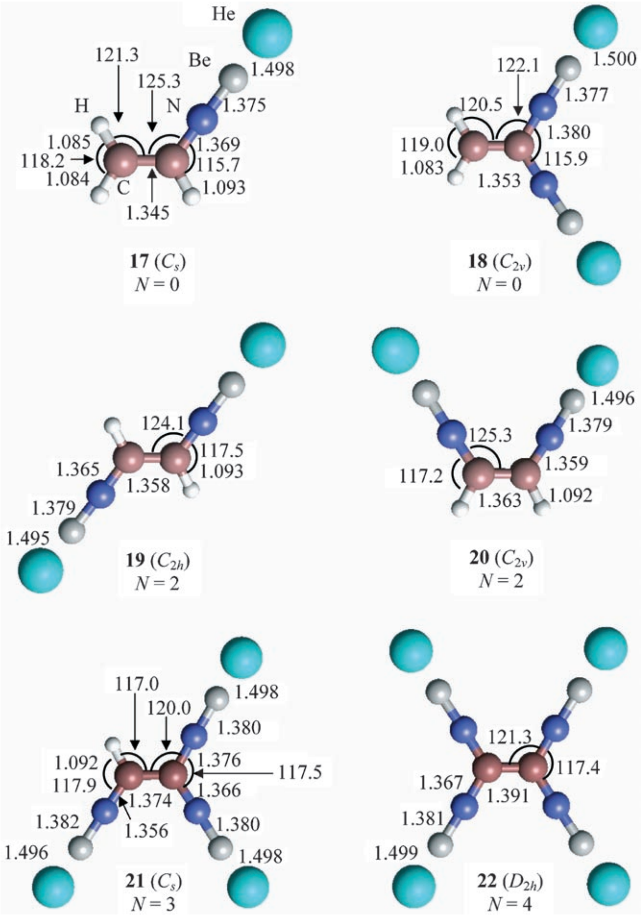

17 (C_s) $N=0$

18 (C_{2v}) $N=0$

19 (C_{2h}) $N=2$

20 (C_{2v}) $N=2$

21 (C_s) $N=3$

22 (D_{2h}) $N=4$

Figure 5. MP2(full)/6-31G(d) optimized geometries (bond lengths in Å and bond angles in °) of the $H_nC_2(NBeHe)_{4-n}$ ($n=0$–3) molecules. N is the number of imaginary frequencies.

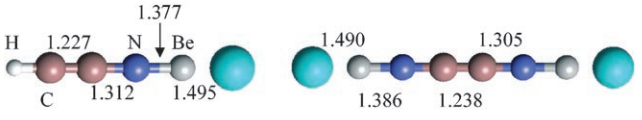

23 ($C_{\infty v}$) $N=0$

24 ($D_{\infty h}$) $N=0$

Figure 6. MP2(full)/6-31G(d) optimized geometries (bond lengths in Å and bond angles in °) of the HC_2NBeHe and $C_2(NBeHe)_2$ molecules. N is the number of imaginary frequencies.

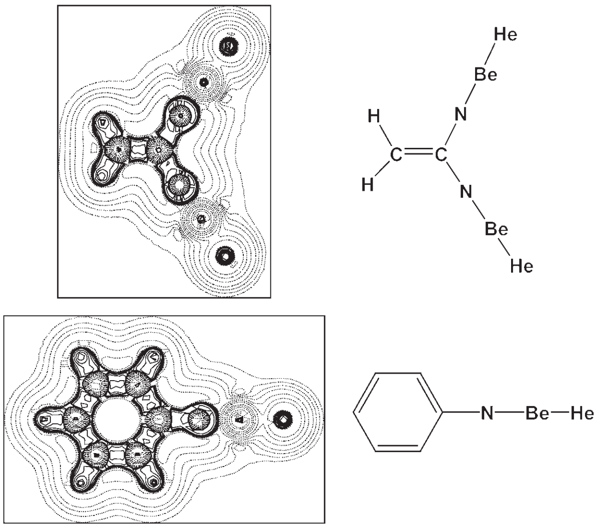

Figure 7. Contour line diagrams of the MP2(full)/6-311G(d,p) Laplacian of the electronic charge density $-\nabla^2\rho(\mathbf{r})$ (in the σ_v plane) of $H_2C_2(NBeHe)_2$ and C_6H_5NBeHe. Dashed lines are in regions of charge depletion ($-\nabla^2\rho(\mathbf{r})<0$) and solid lines in regions of charge concentration ($-\nabla^2\rho(\mathbf{r})>0$).

tivity ($sp^3<sp^2<sp$) of the carbon atom bound to the −NBeHe moiety. The fully linear disubstituted acetylenic complex **24** also revealed a true energy minimum, but the instability of the $C_2(NBeHe)NBe$ fragment on the MP2(full)/6-31G(d) potential-energy surface prevented the evaluation of the fixation energy of the single helium atoms. On the other hand, among the three isomeric complexes $H_2C_2(NBeHe)_2$, only the 1,1-disubstituted structure **18** revealed a true energy minimum, and was stable with respect to the loss of both helium atoms by 4.6 kcal mol^{-1} at the CCSD(T)/6-311G(d,p)//MP2-(full)/6-31G(d) level of theory at 0 K (see Table 7). From Figure 7 and Table 3, similar to

Table 7. MP2(full)/6-31G(d) harmonic vibrational frequencies [cm^{-1}] and CCSD(T)/6-311G(d,p)//MP2(full)/6-31G(d) dissociation energies [kcal mol^{-1}] at 0 K of H_3C_2NBeHe (**17**), $H_2C_2(NBeHe)_2$ (**18**), HC_2NBeHe (**23**), and $C_2(NBeHe)_2$ (**24**) (see Figures 5 and 6).

	H_3C_2NBeHe (**17**)[a]	$H_2C_2(NBeHe)_2$ (**18**)[a]	HC_2NBeHe (**23**)[a]	$C_2(NBeHe)_2$ (**24**)
$\tilde{\nu}$(Be−He)	505.0 (A′,2.5)[b]	442.1 (B_2,9.7)[b]	544.0 (Σ,0.3)[b]	476.3 (Σ_g,0)[b]
		482.8 (A_1,0.04)[b]		565.0 (Σ_u,1.2)[b]
$\tilde{\nu}$(Be−N)	1659.5 (A′,1.9_5)[b]	1247.8 (B_2,204.5)[b]	1686.9 (Σ,37.8_5)[b]	1583.0 (Σ_g, 0)[b]
		1620.3 (A_1,4.2)[b]		1770.3 (Σ_u,24.0)[b]
δ(N-Be-He)	139.4 (A″,7.3)[b]	114.8 (B_1,28.1)[b]	127.0 (∏,5.4)[b]	41.7 ($\prod_u$,48.1)[b]
	139.7 (A′,11.8)[b]	124.2 (A_2,0)[b]		43.3 ($\prod_g$,0)[b]
		138.8 (B_2,5.3)[b]		
		200.8 (A_1,0.6)[b]		
ω(N-Be-He)[c]		90.8 (A_1,24.1)[b]		
$\tilde{\nu}$(C−N)	1764.5 (A′,195.2)[b]	1713.3 (B_2,242.1)[b]	1000.7 (Σ,0.2)[b]	779.9 (Σ_g,0)[b]
		1739.5 (A_1,53.7)[b]		1227.2 (Σ_u,31.0)[b]
δ(C-N-Be)	238.3 (A′,5.7)[b]	211.0 (B_1,8.9)[b]	284.9 (∏,63.1)[b]	110.9 ($\prod_u$,6.4)[b]
	277.3 (A″,14.5)[b]	241.3 (B_2,0.3)[b]		
		276.8 (A_2,0)[b]		
δ(N-C-N)		597.6 (A_1,1.0)[b]		
ΔE_1[d]	4.9 (5.7)[e]	4.6 (5.4)[e]	5.3 (6.0)[e]	
ΔE_2[f]		4.6 (5.4)[e]		

[a] The $-C_2H_n$ motions ($n=1$, 2 or 3) are not included. [b] Symmetry and IR intensity [km mol^{-1}] are given in parentheses. [c] (HeBeN)-C-(NBeHe) bending motion. [d] Energy change of the reactions $H_3C_2NBeHe \rightarrow H_3C_2NBe + He$, $H_2C_2(NBeHe)_2 \rightarrow H_2C_2(NBeHe)NBe + He$, and $HC_2NBeHe \rightarrow HC_2NBe + He$. [e] The values in parentheses are not corrected for the BSSE. [f] Energy change of the reaction $H_2C_2(NBeHe)NBe \rightarrow H_2C_2(NBe)_2 + He$.

the saturated carbon complexes **1**–**4**, the beryllium–helium interaction in **18** is still predicted to be electrostatic.

On the other hand, both the *cis*- and the *trans*-disubstituted structures **19** and **20** are second-order saddle points on the surface, with imaginary frequencies of 45.4i and 48.5i cm^{-1} and 40.6i and 93.8i cm^{-1}, respectively, which refer to the bending motion of the N-Be-He groups and result in the irreversible dissociation of the helium atoms. Similar vibrations and eventual losses of helium atoms are associated with the three imaginary frequencies of structure **21** (92.5i, 114.5i, and 206.7i cm^{-1}) and with the four imaginary frequencies of structure **22** (183.0i, 191.0i, 221.1i, and 243.6i cm^{-1}).

Finally, we have investigated the exemplary aromatic polyhelium complexes formally obtained by replacing the H atoms of C_6H_6 with −NBeHe moieties. Most of the investigated $C_6H_n(NBeHe)_{6-n}$ ($n = 0$–5) molecules, including the largest $C_6(NBeHe)_6$, were actually located as stationary points on the MP2(full)/6-31G(d) potential-energy surface, with Be−N and Be−He bond lengths invariably computed to be around 1.375 and 1.500 Å, respectively. However, only the *ortho*-, *meta*-, and *para*-disubstituted derivatives **26**, **27**, and **28**, respectively, shown in Figure 8 and Table 8 revealed true energy minima, and were stable by approximately 5 $kcal\,mol^{-1}$ with respect to the loss of both the first and the second helium atoms.

The results shown in Figure 7 and Table 3 for the monosubstituted derivative **25** suggest that this interaction is still essentially electrostatic. To investigate the stabilization by the ring substituents of these aromatic helium complexes, we studied the two *para*-disubstituted molecules $HO{-}C_6H_4{-}NBeHe$ and $NC{-}C_6H_4{-}NBeHe$. From Table 3, the results of the AIM analyses of $X{-}C_6H_4{-}NBeHe$ ($X = H$, OH, CN) show only minor differences in the total charges of the relevant C, N, Be, and He atoms, and nearly coincident values of approximately $+8.3\,e\,Å^{-5}$ of the Laplacian of the electron density ($\nabla^2\rho$) at the bond critical point located on the attractor interaction line corresponding to the Be−He bond. Consistently, the CCSD(T)/6-311G(d,p)//MP2(full)/6-31G(d) energy change of the dissociation shown in Equation (12), computed to be 4.9 $kcal\,mol^{-1}$ for $X = H$, resulted in 4.9 $kcal\,mol^{-1}$ for $X = OH$ and 5.1 $kcal\,mol^{-1}$ for $X = CN$.

$$X\text{-}C_6H_4\text{-}NBeHe \rightarrow X\text{-}C_6H_4\text{-}NBe + He \qquad (12)$$

This minor influence of the ring substituent on the stabilization of $X\text{-}C_6H_4\text{-}NBeHe$ refrained us from the computationally more expensive investigation of the conceivable stabilizing effects of aromatic polyhelium complexes by the ring substituents.

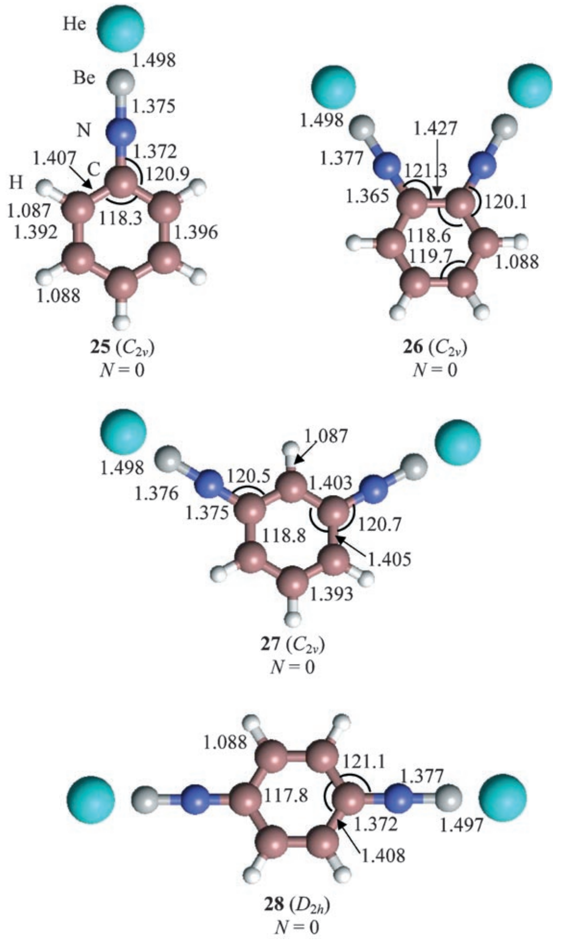

25 (C_{2v}) $N = 0$
26 (C_{2v}) $N = 0$
27 (C_{2v}) $N = 0$
28 (D_{2h}) $N = 0$

Figure 8. MP2(full)/6-31G(d) optimized geometries (bond lengths in Å and bond angles in °) of the C_6H_5NBeHe and $C_6H_4(NBeHe)_2$ molecules. *N* is the number of imaginary frequencies.

Conclusion

Searching for neutral helium compounds still remains a fascinating experimental challenge, and theory is invited to disclose still unexplored features of this chemistry. The results of our ab initio calculations first disclose the conceivable existence of stable or metastable neutral complexes containing more than one (actually up to four) helium atom. This theoretical prediction comes from the recognition that the −NBeHe moiety behaves as a monovalent functional group able to replace the hydrogen atoms of parent molecules to form $M(NBeHe)_n$ ($n > 1$) species of variable size and composition, including, for example, the dihelium complexes $O(NBeHe)_2$, $HP(NBeHe)_2$, and $C_6H_4(NBeHe)_2$, the trihelium complexes $HC(NBeHe)_3$ and $HSi(NBeHe)_3$, and the tetrahelium complexes $C(NBeHe)_4$ and $Si(NBeHe)_4$. All these species were characterized as minimum-energy structures, and featured electrostatic beryllium–helium interactions of approximately 4–5 $kcal\,mol^{-1}$. On the other hand, complexes such as $HN(NBeHe)_2$, $S(NBeHe)_2$, $C_2(NBeHe)_4$, and $C_6(NBeHe)_6$ were characterized as high-order saddle points, and were unstable with respect to the loss of helium atoms owing to the bending of the −NBeHe groups. Therefore, it cannot be safely predicted that any $M(NBeHe)_n$ ($n > 1$) structure actually resides in a potential energy well. This consideration, however, does not undermine the suggestion that the class of $M(NBeHe)_n$ ($n > 1$) polyhelium complexes

Table 8. MP2(full)/6-31G(d) harmonic vibrational frequencies [cm^{-1}] and CCSD(T)/6-311G(d,p)//MP2(full)/6-31G(d) dissociation energies [kcal mol^{-1}] at 0 K of the $C_6H_{6-n}(NBeHe)_n$ ($n=1, 2$) molecules **25**–**28** (see Figure 8).

	C_6H_5NBeHe (**25**)[a]	*o*-$C_6H_4(NBeHe)_2$ (**26**)[a]	*m*-$C_6H_4(NBeHe)_2$ (**27**)[a]	*p*-$C_6H_4(NBeHe)_2$ (**28**)[a]
$\tilde{\nu}$(Be–He)	596.0 (A_1,6.0)[b]	561.6 (B_2,3.6)[b]	594.9 (B_2,11.3)[b]	508.3 (B_{1u},3.4)[b]
		614.2 (A_1,4.7)[b]	604.0 (A_1,1.4)[b]	589.2 (A_g,0)[b]
$\tilde{\nu}$(Be–N)	1667.6 (A_1,8.3)[b]	1518.1 (A_1,27.0)[b]	1521.8 (B_2,63.5)[b]	1528.1 (B_{1u},95.3)[b]
		1654.7 (B_2,4.1)[b]	1632.4 (A_1,5.1)[b]	1656.8 (A_g,0)[b]
δ(N-Be-He)	177.2 (B_1,0.7)[b]	108.5 (B_2,22.6)[b]	101.2 (A_2,0)[b]	93.0 (B_{2g},0)[b]
	213.1 (B_2,1.6)[b]	126.9 (A_2,0)[b]	119.2 (B_2,7.6)[b]	119.9 (B_{3g},0)[b]
		145.0 (B_1,9.2)[b]	161.1 (B_1,0.001)[b]	123.2 (B_{3u},4.4)[b]
		178.8 (A_1,0.4)[b]	218.4 (B_2,1.1)[b]	199.0 (B_{2u},0.05)[b]
ω(N-Be-He)[c]	99.5 (B_1,16.6)[b]	77.1 (A_2,0)[b]	83.4 (A_1,23.3)[b]	58.3 (B_{3u},32.0)[b]
	109.9 (B_2,15.5)[b]	81.7 (B_1,29.6)[b]	88.1 (B_1,34.5)[b]	86.1 (B_{2u},33.5)[b]
		83.0 (A_1,6.1$_5$)[b]		
$\tilde{\nu}$(C–N)	1746.3 (A_1,263.4)[b]	1721.9 (A_1,148.6)[b]	1734.4 (B_2,378.9)[b]	1728.7 (A_g,0)[b]
		1742.4 (B_2,123.9)[b]	1736.4 ($A_{1,}$67.7)[b]	1738.8 (B_{1u},408.6)[b]
δ(C-N-Be)	306.9 (B_1,5.6)[b]	213.5 (B_2,3.4)[b]	302.7 (A_2,0)[b]	184.7 (B_{2g},0)[b]
	482.9 (B_2,2.8)[b]	248.3 (A_2,0)[b]	409.7 (A_1,3.7)[b]	219.2 (B_{3g},0)[b]
		397.3 (A_1,1.9)[b]	445.0 (A_1,2.0)[b]	281.4 (B_{3u},12.8)[b]
		482.0 (B_1,1.4)[b]	538.5 (B_1,0.2)[b]	445.8 (B_{2u},6.9)[b]
ΔE_1[d]	4.9 (5.7)[e]		4.8 (5.6)[e]	4.8 (5.6)[e]
ΔE_2[f]			4.9 (5.7)[e]	4.8 (5.6)[e]

[a] The $-C_6H_n$ motions ($n=4$ or 5) are not included. [b] Symmetry and IR intensity [km mol^{-1}] are given in parentheses. [c] C-C-(NBeHe) bending motion. [d] Energy change of the reactions $C_6H_5NBeHe \rightarrow C_6H_5NBe + He$ and $C_6H_4(NBeHe)_2 \rightarrow C_6H_4(NBeHe)NBe + He$. [e] The values in parentheses are not corrected for the BSSE. [f] Energy change of the reaction $C_6H_4(NBeHe)NBe \rightarrow C_6H_4(NBe)_2 + He$.

may, in principle, be very large, and, if anything, invites a more detailed investigation of the factors that control their detailed structure and stability.

Computational Methods

The quantum chemical calculations were performed by using Unix versions of the Gaussian 98[44] and MOLPRO 2000.1[45] sets of programs installed on an Alphaserver 1200 and a DS20E Compaq machine. The geometries of all the investigated species were optimized, by using the 6-31G(d) basis set,[46] at the second-order Møller–Plesset level of theory with inclusion of the inner electrons, MP2(full),[47] and the obtained structures were characterized as true minima or higher-order saddle points by calculation of the MP2(full)/6-31G(d) vibrational frequencies. The zero-point vibrational energies (ZPE) were also obtained in this way. The MP2(full)/6-31G(d) geometries were subsequently used to perform single-point calculations at the Coupled Cluster level of theory (frozen-core approximation), including the contribution from single and double substitutions and an estimate of connected triples, CCSD(T),[48,49] with the 6-311G(d,p) basis set.[46] The geometry of $H_2C(NBeHe)_2$ was also refined at the MP2(full), CCD, and CCSD(T) levels of theory by using the larger basis sets 6-311G(d,p) and 6-311++G(2df,2p).[46] At the CCSD(T) level of theory, the T1 diagnostic was calculated according to Lee and Taylor,[50] and the dissociation energies were corrected for the basis-set superposition error (BSSE) by using the method by Boys and Bernardi.[51] Chemical bonding analysis was based on the theory of Atoms-in-Molecules (AIM),[52] by using the implementation in Gaussian 98 developed by Cioslowski and co-workers,[53,54] and the AIM2000 program package.[55] In particular, we have calculated the MP2(full)/6-311G(d,p) total charges (q), the charge density (ρ), and the Laplacian of the charge density ($\nabla^2\rho$) at the bond critical points (bcp), intended to be the points on the attractor interaction lines where $\nabla^2\rho=0$, and the covalent bond order of the various chemical bonds.

Acknowledgements

We thank the Italian Ministero dell' Istruzione, dell' Università e della Ricerca (MIUR) and the Consiglio Nazionale delle Ricerche (CNR) for financial support.

---

[1] N. Bartlett, *Proc. Chem. Soc.* **1962**, 218.
[2] L. Graham, O. Graudejus, N. K. Jha, N. Bartlett, *Coord. Chem. Rev.* **2000**, *197*, 321.
[3] J. J. Turner, G. C. Pimentel, *Science* **1963**, *140*, 974.
[4] F. A. Cotton, G. Wilkinson, *Advanced Inorganic Chemistry*, Wiley, New York, **1999**.
[5] S. Seidel, K. Seppelt, *Science* **2000**, *290*, 117.
[6] P. Pyykkö, *Science* **2000**, *290*, 64.
[7] K. O. Christe, *Angew. Chem.* **2001**, *113*, 1465; *Angew. Chem. Int. Ed.* **2001**, *40*, 1419.
[8] L. Andrews, B. Liang, J. Li, B. E. Bursten, *J. Am. Chem. Soc.* **2003**, *125*, 3126.
[9] H. Tanskanen, L. Khriachtchev, J. Lundell, H. Kiljunen, M. Räsänen, *J. Am. Chem. Soc.* **2003**, *125*, 16361.
[10] G. Tavčar, P. Benkič, B. Žemva, *Inorg. Chem.* **2004**, *43*, 1452.
[11] J. M. Michaud, S. A. Cooke, M. C. L. Gerry, *Inorg. Chem.* **2004**, *43*, 3871.
[12] L. Khriachtchev, M. Pettersson, N. Runeberg, J. Lundell, M. Räsänen, *Nature* **2000**, *406*, 874.
[13] G. Frenking, *Nature* **2000**, *406*, 836.
[14] J. R. Wells, E. Weitz, *J. Am. Chem. Soc.* **1992**, *114*, 2783.
[15] X.-Z. Sun, M. W. George, S. G. Kazarian, S. M. Nikiforov, M. Poliakoff, *J. Am. Chem. Soc.* **1996**, *118*, 10525.
[16] A. W. Ehlers, G. Frenking, E. J. Baerends, *Organometallics* **1997**, *16*, 4896.
[17] C. A. Thompson, L. Andrews, *J. Am. Chem. Soc.* **1994**, *116*, 423.
[18] C. J. Evans, M. C. L. Gerry, *J. Chem. Phys.* **2000**, *112*, 1321.
[19] C. J. Evans, M. C. L. Gerry, *J. Chem. Phys.* **2000**, *112*, 9363.
[20] C. J. Evans, D. S. Rubinoff, M. C. L. Gerry, *Phys. Chem. Chem. Phys.* **2000**, *2*, 3943.

[21] C. J. Evans, A. Lesarri, M. C. L. Gerry, *J. Am. Chem. Soc.* **2000**, *122*, 6100.
[22] J. Li, B. E. Bursten, B. Liang, L. Andrews, *Science* **2002**, *295*, 2242.
[23] G. Frenking, D. Cremer, *Struct. Bonding (Berlin)* **1990**, *73*, 17.
[24] *CRC Handbook of Chemistry and Physics*, 74th ed. (Ed.: D. R. Lide), CRC Press, Boca Raton, **1993**.
[25] F. Grandinetti, *Int. J. Mass Spectrom.* **2004**, *237*, 243.
[26] J. P. Toennies, A. F. Vilesov, *Angew. Chem.* **2004**, *116*, 2674; *Angew. Chem. Int. Ed.* **2004**, *43*, 2622.
[27] J. J. Manley, *Nature* **1925**, *115*, 337.
[28] R. Heller, *J. Chem. Phys.* **1941**, *9*, 154.
[29] T. Weiske, T. Wong, W. Krätschmer, J. K. Terlow, H. Schwarz, *Angew. Chem.* **1992**, *104*, 242; *Angew. Chem. Int. Ed. Engl.* **1992**, *31*, 183.
[30] M. Saunders, H. A. Jiménez-Vázquez, R. J. Cross, R. J. Poreda, *Science* **1993**, *259*, 1428.
[31] M. W. Wong, *J. Am. Chem. Soc.* **2000**, *122*, 6289.
[32] G. M. Chaban, J. Lundell, R. B. Gerber, *J. Chem. Phys.* **2001**, *115*, 7341.
[33] T. Takayanagi, A. Wada, *Chem. Phys. Lett.* **2002**, *352*, 91.
[34] Z. Bihary, G. M. Chaban, R. B. Gerber, *J. Chem. Phys.* **2002**, *117*, 5105.
[35] A. Lignell, L. Khriachtchev, M. Rasanen, M. Pettersson, *Chem. Phys. Lett.* **2004**, *390*, 256.
[36] S. A. C. McDowell, *Chem. Phys. Lett.* **2004**, *396*, 346.
[37] S. Borocci, N. Bronzolino, F. Grandinetti, *Chem. Phys. Lett.* **2005**, *406*, 179.
[38] J. Baker, P. W. Fowler, A. Soncini, M. Lillington, *J. Chem. Phys.* **2005**, *123*, 174309.
[39] W. Koch, J. R. Collins, G. Frenking, *Chem. Phys. Lett.* **1986**, *132*, 330.
[40] W. Koch, G. Frenking, J. Gauss, D. Cremer, J. R. Collins, *J. Am. Chem. Soc.* **1987**, *109*, 5917.
[41] G. Frenking, W. Koch, J. Gauss, D. Cremer, *J. Am. Chem. Soc.* **1988**, *110*, 8007.
[42] S. Borocci, N. Bronzolino, F. Grandinetti, *Chem. Phys. Lett.* **2004**, *384*, 25.
[43] P. Antoniotti, N. Bronzolino, F. Grandinetti, *J. Phys. Chem. A* **2003**, *107*, 2974.
[44] Gaussian 98 (Revision A.7), M. J. Frisch, G. W. Trucks, H. B. Schlegel, G. E. Scuseria, M. A. Robb, J. R. Cheeseman, V. G. Zakrzewski, J. A. Montgomery, Jr., R. E. Stratmann, J. C. Burant, S. Dapprich, J. M. Millam, A. D. Daniels, K. N. Kudin, M. C. Strain, O. Farkas, J. Tomasi, V. Barone, M. Cossi, R. Cammi, B. Mennucci, C. Pomelli, C. Adamo, S. Clifford, J. Ochterski, G. A. Petersson, P. Y. Ayala, Q. Cui, K. Morokuma, D. K. Malick, A. D. Rabuck, K. Raghavachari, J. B. Foresman, J. Cioslowski, J. V. Ortiz, B. B. Stefanov, G. Liu, A. Liashenko, P. Piskorz, I. Komaromi, R. Gomperts, R. L. Martin, D. J. Fox, T. Keith, M. A. Al-Laham, C. Y. Peng, A. Nanayakkara, C. Gonzalez, M. Challacombe, P. M. W. Gill, B. G. Johnson, W. Chen, M. W. Wong, J. L. Andres, M. Head-Gordon, E. S. Replogle, J. A. Pople, Gaussian, Inc., Pittsburgh, PA, **1998**.
[45] MOLPRO is a package of ab initio programs written by H.-J. Werner and P. J. Knowles, with contributions from R. D. Amos, A. Bernhadsson, A. Berning, P. Celani, D. L. Cooper, M. J. O. Deegan, A. J. Dobbyn, F. Eckert, C. Hampel, G. Hetzer, T. Korona, R. Lindh, A. W. Lloyd, S. J. McNicholas, F. R. Manby, W. Meyer, M. E. Mura, A. Nicklass, P. Palmieri, R. Pitzer, G. Rauhut, M. Schatz, H. Stoll, A. J. Stone, R. Tarroni, and T. Thorsteinsson.
[46] W. J. Hehre, L. Radom, P. von R. Schleyer, J. A. Pople, *Ab Initio Molecular Orbital Theory*, Wiley, New York, **1986**.
[47] C. Møller, M. S. Plesset, *Phys. Rev.* **1934**, *46*, 618.
[48] K. Raghavachari, G. W. Trucks, J. A. Pople, M. Head-Gordon, *Chem. Phys. Lett.* **1989**, *157*, 479.
[49] C. Hampel, K. Peterson, H.-J. Werner, *Chem. Phys. Lett.* **1992**, *190*, 1.
[50] T. J. Lee, P. R. Taylor, *Int. J. Quantum Chem. Quantum Chem. Symp.* **1989**, *23*, 199.
[51] S. Boys, F. Bernardi, *Mol. Phys.* **1970**, *19*, 553.
[52] R. F. W. Bader, *Atoms in Molecules: A Quantum Theory*, Oxford University Press, Oxford, **1990**.
[53] J. Cioslowski, S. T. Mixon, *J. Am. Chem. Soc.* **1991**, *113*, 4142.
[54] J. Cioslowski, A. Nanayakkara, *Chem. Phys. Lett.* **1994**, *219*, 151.
[55] AIM2000, designed by F. Biegler-König, University of Applied Sciences, Bielefeld, Germany (http://www.AIM2000.de).

Received: February 16, 2006